On energy transfer of parametric resonance for wave energy conversion

Bingyong Guo, John V. Ringwood

***Abstract*—Parametric resonance has been observed, both numerically and experimentally, in various studies of wave energy converters (WECs). Large heave motions induce a periodic variation in the metacentric height of a WEC body and, consequently, cause a harmonic variation in pitch/roll restoring coefficients, which can parametrically excite the pitch/roll modes. Current studies attempt to determine the occurrence conditions of parametric resonance, by detecting the boundaries between stable and unstable regions in the parameter space. In the literature, some studies aim to make use of parametric resonance for improving power capture. In contrast, some studies try to suppress the effect of parametric resonance, as it can reduce power capture efficiency in the primary degree of freedom. However, how energy transfers from one mode to another is not fully understood. This study aims to analyse energy transfer between heave and pitch/roll modes when parametric resonance occurs. A generic cylindrical point absorber is studied as a WEC floater to consider non-linear wave-structure interaction, including non-linear Froude-Krylov and viscous forces. A heave-pitch-roll three-degree-of-freedom model is derived for numerical study of the energy transfer between different operational modes.**

***Index Terms*—Wave energy converter, parametric resonance, energy transfer, multiple degrees of freedom, hydrodynamic modelling**

I. Introduction

Parametric resonance is widely observed in engineering practice, viewed as beneficial for the design of micro-electromechanical systems (MEMSs) [1] and energy harvesting systems [2], but treated as a harmful phenomenon in ocean engineering, potentially causing large undesired roll/pitch motion for ships and offshore platforms. For ships, parametric resonance in roll is mainly due to the variation of the ship metacentric height, induced by large heave motion, resulting in exaggerated roll motion, even to the point of capsizing. To suppress parametric ship roll resonance, various passive and active control approaches, e.g. utilising fins or U-tanks, and manoeuvring cruise speed or yaw angle, are discussed in [3]. Spar-shaped offshore platforms are also prone to parametric resonance, both in roll and pitch, mainly due to their relatively large draft.

Parametric resonance has also been observed, both numerically and experimentally, in various studies of wave energy converters (WECs), e.g. oscillating water columns (OWCs) [4]–[7] and point absorbers (PAs) [8], [9]. Large heave motion induces a periodic variation in the metacentric height of a WEC body and, consequently, causes a dynamic variation in pitch/roll restoring coefficients, which can parametrically excites the pitch/roll modes. Under certain conditions, e.g. where the incident wave frequency is twice the pitch/roll natural frequency, parametric resonance occurs in pitch/roll modes and causes the pitch/roll motion to increase exponentially, known as the Mathieu instability [10].

However, the onset conditions of parametric resonance for offshore structures is more complex than that of Mathieu's instability, since the hydrodynamics are highly nonlinear and implicit. In addition, the occurrence, and demonstration, of parametric resonance also significantly relies on the mass distribution [11], mooring design [12], [13], structure geometry [5], [14], [15], and hydrodynamic modelling methods [6], [9], [15]–[17].

Mathieu's equation [10] is generally used to explain the occurrence of parametric resonance, mainly assuming that heave motion is known or recorded [5], [11]. Thus, the variation of the metacentric height is expressed as a function of heave and then parametrically excites the roll/pitch motions. However, experimental results indicates that the coupling between heave and roll/pitch is bi-directional [5], [16]–[18]. Since the coupling between various degrees of freedom (DoFs) is highly nonlinear, computational fluid dynamics (CFD) modelling in OpenFOAM has been applied to depict heave-roll-pitch interaction for a truncated cylinder and a cylinder with a smooth hemispherical bottom in [15], which reveals the importance of viscous effect on parametric resonance. As expected, CFD modelling is expensive in computing time and effort. In addition, hybrid modelling methods, considering nonlinear Froude-Krylov (FK) forces with respect to instantaneous wetted surface, are utilised in some studies [6], [17], [19].

Current studies attempt to determine the occurrence conditions for parametric resonance, by detecting the boundaries between stable and unstable regions in the parameter space. However, there are only a few studies investigating the energy transfer from one mode to another. Some studies try to suppress the effect of parametric resonance [5], [7], since it can reduce power capture efficiency, while other studies aim to make use of parametric resonance for improving power capture [4], [9]. For spar-buoy OWC devices, parametric resonance can be suppressed by passive fins [5] or actively controlled pressure relief valves [20]. However, how energy transfers from one mode to another is still not fully understood.

This study aims to analyse the energy transfer between heave and roll/pitch modes when parametric

B. Guo and J.V. Ringwood are with Centre for Ocean Energy Research, Maynooth University, Ireland (e-mail: bingyong.guo@mu.ie,john.ringwood@mu.ie).

resonance occurs, using the hybrid modelling method and corresponding open-access toolbox developed in [6], [19]. Without loss of generality, a generic cylindrical point absorber is studied as a WEC floater to consider non-linear wave-structure interaction, including non-linear FK and viscous forces. A heave-roll-pitch 3-DoF model is derived for the numerical study of parametric resonance, with specific foci on mutual (bi-directional) interaction, viscous effects, multi-stability and energy transfer between different DoFs.

The reminder of the paper is organised as follows: Section II discusses Mathieu's equation for modelling parametric resonance. Linear modelling of the heave-roll-pitch 3-DoF PA is discussed in Section III, with the hybrid modelling method, considering nonlinear FK and viscous forces, described in Section IV. Numerical results are presented and discussed in Section V. Finally, Section VI draws some conclusions and indicates potential future work.

II. Mathieu Instability

Mathieu's equation is widely used to explain the onset and instability of parametric resonance. A good example is the spar-buoy OWC device, where parametric resonance in roll is observed numerically and experimental [5]. As Mathieu's equation to model parametric resonance is well described in [5], just an overview is given here, as follows. For heave-induced parametric resonance in roll, Mathieu's equation is given as

$$\frac{\mathrm{d}^2\xi_4}{\mathrm{d}\tau^2} + c\frac{\mathrm{d}\xi_4}{\mathrm{d}\tau} + [\delta + \epsilon\cos(\tau)]\xi_4 = 0, \tag{1}$$

where ξ_4 is the roll angle, and $\tau = \omega t$ is the time index for Mathieu's equation. c, δ and ϵ are the non-dimensional damping, stiffness and parametric excitation amplitude, respectively, given as

$$c = \frac{B_{44}}{\omega(M_{44}+A_{44})}, \tag{2}$$

$$\delta = (\frac{\omega_{n4}}{\omega})^2, \tag{3}$$

$$\epsilon = \frac{|\hat{\xi}_3|}{\overline{GM}_0}(\frac{\omega_{n4}}{\omega})^2, \tag{4}$$

$$\omega_{n4} = \sqrt{\frac{\rho g V_\mathrm{d}\overline{GM}_0}{M_{44}+A_{44}}}, \tag{5}$$

where M_{44}, A_{44}, B_{44}, K_{44} are the inertia, added mass, radiation damping and hydrostatic stiffness in roll, respectively, dependent on the hull geometry and wave frequency ω. ω_{n4} is the natural frequency in roll, as a function of the displaced volume V_d, average metacentric height $\overline{GM}_0$, and the total inertia $M_{44}+A_{44}$. ρ and g are the water density and gravitational acceleration constants, respectively. It is worth noting that the amplitude of the heave motion, $|\hat{\xi}_3|$, is assumed known.

As a classical differential equation, a systematic overview of Mathieu's equation is given in [10], with specific foci on its stability, non-linear extension, bifurcation and co-existence. The Mathieu-type instability in the $\delta-\epsilon$ parameter space is shown in Fig. 1, where δ and ϵ represent the frequency and amplitude

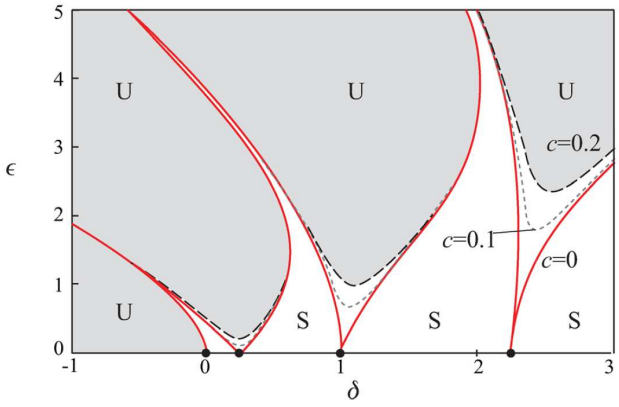

Fig. 1. Instability chart of Mathieu's equation in Eq. (1), adopted from [10].

conditions, respectively. For parameters in the unstable (or shadowed) region, the roll motion increases exponentially to infinity, characteristic of the Mathieu instability.

Though Mathieu's equation is useful to explain the onset of parametric resonance, there are some drawbacks for WEC modelling: (i) Mathieu's equation in Eq. (1) only considers a linear damping term, and roll motion increases exponentially to infinity. In practice, a large roll motion induces some non-linear terms, e.g. quadratic or cubic damping term or stiffness, which can limit the maximum roll angle [10], [21], [22]. (ii) The motion in heave is assumed known or prescribed, and such information is needed in computing ϵ in Eq. (4). This is not always the case for WEC modelling. (iii) Mathieu's equation can only reflect the influence of heave motion on roll motion. However, this is part of the parametric coupling story. In fact, heave and roll motions are *mutually* coupled [16], and Mathieu's equation cannot express the influence of parametric resonance in roll on the heave mode.

This study utilises a hybrid modelling method to study the mutual interaction between heave, roll and pitch modes, by considering non-linear FK forces, to investigate quadratic viscous effects on parametric resonance by adding the Morison drag term to the linear model, and to discuss the influence of parametric resonance on WEC power absorption by applying passive control.

III. Linear Modelling

As linear hydrodynamic modelling is the foundation of the hybrid modelling method, this section gives an overview of WEC linear hydrodynamics. A simple cylindrical PA is used in this study, with a radius of $R = 2$ m, a height of $H = 8$ m, a draft of $d = 6$ m, and a centre of gravity of $CoG = (0, 0, -3.1)$ m, as shown in Fig. 2. The water depth is assumed as $h = 100$ m.

The dynamics of the cylindrical PA in Fig. 2 are governed by Newton's 2^{nd} Law, given as

$$\boldsymbol{M}\ddot{\boldsymbol{\xi}}(t) = \boldsymbol{f}_\mathrm{h}(t) + \boldsymbol{f}_\mathrm{g}(t) + \boldsymbol{f}_\mathrm{pto}(t), \tag{6}$$

where $\boldsymbol{M}$ is the PA inertial matrix and $\boldsymbol{\xi}$ is the PA displacement matrix. $\boldsymbol{f}_\mathrm{h}$, $\boldsymbol{f}_\mathrm{g}$ and $\boldsymbol{f}_\mathrm{pto}$ are the hydrodynamic, gravity and PTO (or control) forces, respectively.

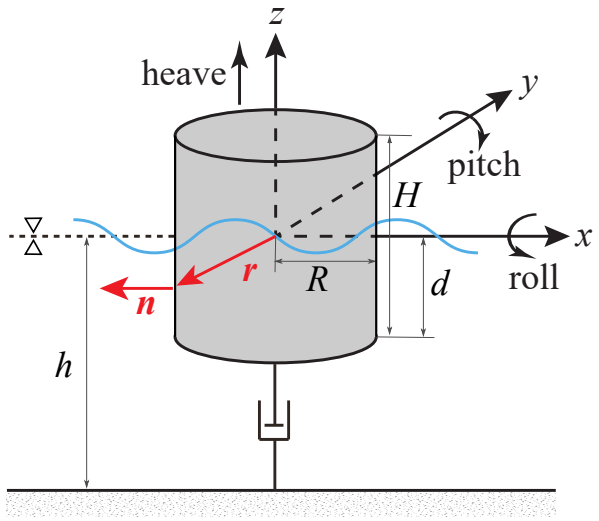

Fig. 2. Geometric of a cylindrical point absorber in heave-roll-pitch motion.

These parameters or variables contain heave, roll and pitch components, as illustrated in Fig. 2. The time variable t is omitted in what follows, for brevity.

Based on linear potential flow theory, the hydrodynamic force $\boldsymbol{f}_{\mathrm{h}}$ can be expressed as

$$\boldsymbol{f}_{\mathrm{h}} = \boldsymbol{f}_{\mathrm{fk,dy}} + \boldsymbol{f}_{\mathrm{fk,hs}} + \boldsymbol{f}_{\mathrm{d}} + \boldsymbol{f}_{\mathrm{r}}, \tag{7}$$

where $\boldsymbol{f}_{\mathrm{fk,dy}}$ and $\boldsymbol{f}_{\mathrm{fk,st}}$ represent the dynamic and static FK forces, respectively. $\boldsymbol{f}_{\mathrm{d}}$ and $\boldsymbol{f}_{\mathrm{r}}$ are the diffraction and radiation forces, respectively.

The sum of the dynamic FK force and the diffraction force is defined as the excitation force, given as

$$\boldsymbol{f}_{\mathrm{e}} = \boldsymbol{f}_{\mathrm{fk,dy}} + \boldsymbol{f}_{\mathrm{d}}. \tag{8}$$

In addition, the sum of the static FK and gravity forces is called hydrostatic (or restoring) force, which is proportional to the PA displacement, given as

$$\boldsymbol{f}_{\mathrm{hs}} = \boldsymbol{f}_{\mathrm{fk,hs}} + \boldsymbol{f}_{\mathrm{g}} = -\boldsymbol{K}\boldsymbol{\xi}, \tag{9}$$

where $\boldsymbol{K}$ is the hydrostatic stiffness. It is worth mentioning that $\boldsymbol{f}_{\mathrm{fk,hs}} + \boldsymbol{f}_{\mathrm{g}} = 0$ holds when the body is at its equilibrium point in still water. The radiation force can be expressed as

$$\boldsymbol{f}_{\mathrm{r}} = -\boldsymbol{A}_{\infty}\ddot{\boldsymbol{\xi}} - \boldsymbol{k}_{\mathrm{r}} * \dot{\boldsymbol{\xi}}, \tag{10}$$

where $\boldsymbol{A}_{\infty}$ is the added mass at infinite frequency, and $\boldsymbol{k}_{\mathrm{r}}$ is the impulse response function (IRF) associated with the radiation force. $*$ is the convolution operator.

Substituting Eqs. (7)-(10) into Eq. (6), the WEC dynamics can be rewritten as the well-known Cummins' equation, given as

$$\boldsymbol{M}\ddot{\boldsymbol{\xi}} = \boldsymbol{f}_{\mathrm{e}} + \boldsymbol{f}_{\mathrm{r}} + \boldsymbol{f}_{\mathrm{hs}} + \boldsymbol{f}_{\mathrm{pto}}. \tag{11}$$

In the frequency-domain, Cummins' equation in Eq. (11) can be rewritten as

$$\{-\omega^2[\boldsymbol{M} + \boldsymbol{A}] + j\omega\boldsymbol{B} + \boldsymbol{K}\}\boldsymbol{\Xi}(\omega) = \boldsymbol{F}_{\mathrm{e}}(\omega) + \boldsymbol{F}_{\mathrm{pto}}(\omega), \tag{12}$$

where $\boldsymbol{\Xi}(\omega)$ and $\boldsymbol{F}_{\mathrm{e}}(\omega)$ are the frequency-domain representations of $\boldsymbol{\xi}(t)$ and $\boldsymbol{f}_{\mathrm{e}}(t)$, respectively. $\boldsymbol{F}_{\mathrm{pto}}(\omega)$ represents the control force. $\boldsymbol{A}$ and $\boldsymbol{B}$ are the added mass and radiation damping, respectively.

To derive the passive control solution, Cummins' equation in Eq. (12) can be rewritten as

$$\frac{\boldsymbol{V}(\omega)}{\boldsymbol{F}_{\mathrm{e}}(\omega) + \boldsymbol{F}_{\mathrm{pto}}(\omega)} = \frac{1}{\boldsymbol{Z}_{\mathrm{i}}(\omega)}, \tag{13}$$

where $\boldsymbol{V}(\omega)$ represents the body velocity, $\dot{\boldsymbol{\xi}}(t)$, in the frequency domain. $\boldsymbol{Z}_{\mathrm{i}}(\omega)$ is the intrinsic impedance of the system, given as

$$\boldsymbol{Z}_{\mathrm{i}}(\omega) = \boldsymbol{B}(\omega) + j\omega\left[\boldsymbol{M} + \boldsymbol{A}(\omega) - \frac{\boldsymbol{K}}{\omega^2}\right]. \tag{14}$$

Thus, the passive control (PC) [23] solution can be expressed as

$$\boldsymbol{B}_{\mathrm{pto}}(\omega) = |\boldsymbol{Z}_{\mathrm{i}}(\omega)|, \tag{15}$$

where $\boldsymbol{B}_{\mathrm{pto}}$ is the PTO damping coefficient for PC implementation. For a given wave frequency ω, the PTO force is given as

$$\boldsymbol{f}_{\mathrm{pto}} = -\boldsymbol{B}_{\mathrm{pto}}\dot{\boldsymbol{\xi}}. \tag{16}$$

To quantify the power and energy captured from wave by the PA, the excitation power and energy are defined, respectively,as

$$\boldsymbol{P}_{\mathrm{e}} = \boldsymbol{f}_{\mathrm{e}}\dot{\boldsymbol{\xi}}, \tag{17}$$

$$\boldsymbol{E}_{\mathrm{e}} = \int_0^T \boldsymbol{P}_{\mathrm{e}}\ \mathrm{d}t, \tag{18}$$

where T is the integral time span. Similar, the absorbed power and energy by the PTO damper are defined, respectively, as

$$\boldsymbol{P}_{\mathrm{pto}} = -\boldsymbol{f}_{\mathrm{pto}}\dot{\boldsymbol{\xi}}, \tag{19}$$

$$\boldsymbol{E}_{\mathrm{pto}} = \int_0^T \boldsymbol{P}_{\mathrm{pto}}\ \mathrm{d}t. \tag{20}$$

In this study, the boundary element method (BEM) toolbox NEMOH is used, to obtain $\boldsymbol{M}$, $\boldsymbol{A}_{\infty}$, $\boldsymbol{A}$, $\boldsymbol{B}$, $\boldsymbol{K}$ and k_{r} directly. In NEMOH, the frequency ranges from 0.1 rad/s to 6 rad/s with an interval of 0.1 rad/s. In Eq. (10), the convolution term, $\boldsymbol{k}_{\mathrm{r}} * \dot{\boldsymbol{\xi}}$, is neither straightforward nor computationally efficient in WEC modelling and control. Thus, it is approximated by a finite-order state-space model using the time-domain methods in [24], [25], with the results show in Figs. 3(a)-(b). Alternatively, it can also be approximated by frequency-domain methods, as discussed in [26]–[28].

NEMOH can only give the frequency response function of the excitation force, $\boldsymbol{K}_{\mathrm{e}}(\omega)$ (representing the systematic property of physical process from wave elevation to wave excitation force), and, thus, its IRF, $\boldsymbol{k}_{\mathrm{e}}(t)$ can be computed according to

$$\boldsymbol{k}_{\mathrm{e}}(t) = \frac{1}{2\pi}\int_{-\infty}^{\infty} \boldsymbol{K}_{\mathrm{e}}(\omega)e^{j\omega t}\mathrm{d}\omega. \tag{21}$$

Thus, the excitation force, in the time domain, can be expressed as

$$\boldsymbol{f}_{\mathrm{e}}(t) = \boldsymbol{k}_{\mathrm{e}}(t) * \eta(t), \tag{22}$$

where $\eta(t)$ is the incident wave. However, the excitation IRF is known to be non-causal, shown in Figs. 4(a)-(b). The approximation of the convolution

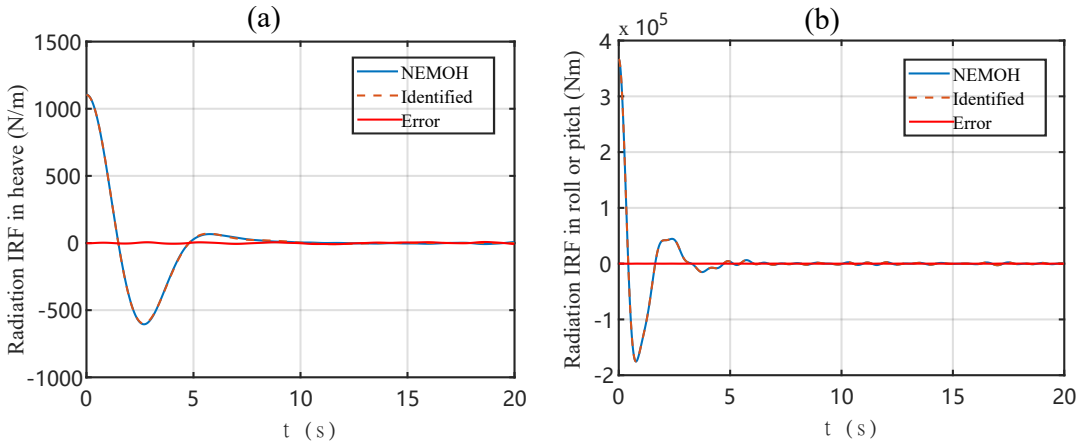

Fig. 3. Radiation approximation in (a) heave and (b) roll/pitch motions, respectively.

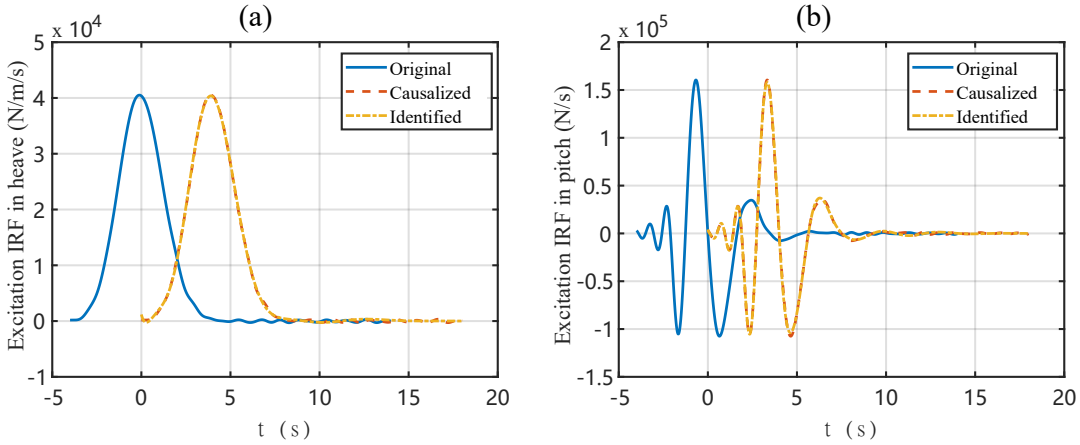

Fig. 4. Excitation approximation in (a) heave and (b) pitch motions, respectively.

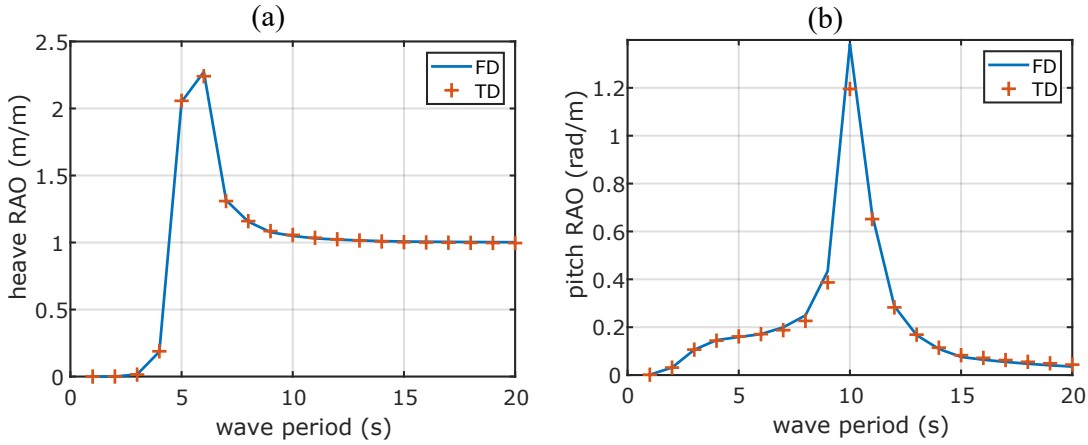

Fig. 5. Comparison between the time- and frequency-domains liner models in terms of response amplitude operation (RAO) in (a) heave, and (b) pitch modes, respectively.

term, $\boldsymbol{k}_{\mathrm{e}}(t) * \eta(t)$ is not as straightforward as the radiation approximation. In the literature, a variety of methods are applied to approximate or estimate the excitation force [29]–[32]. In this study, the excitation force approximation proposed in [30], [31] is adopted to derive a time domain model.

By approximating the radiation and excitation forces, a time-domain model for Cummins' equation is obtained, and its response amplitude operator (RAO) with various wave periods is compared with the frequency-domain counterpart in Fig. 5.

IV. Non-linear modelling

To investigate the mutual interaction between multiple DoFs, a hybrid modelling method is used to augment the linear Cummins' equation in Eq. (11) with some critical non-linear forces. In this study, the non-linear FK force with respect to the instantaneous wetted surface, and the viscous force represented by the quadratic drag term in the Morison equation, are added to Eq. (11) as non-linear treatments, given as

$$\boldsymbol{M}\ddot{\boldsymbol{\xi}} = \boldsymbol{f}_{\mathrm{nlfk,dy}} + \boldsymbol{f}_{\mathrm{nlfk,st}} + \boldsymbol{f}_{\mathrm{d}} + \boldsymbol{f}_{\mathrm{r}} + \boldsymbol{f}_{\mathrm{g}} + \boldsymbol{f}_{\mathrm{pto}} + \boldsymbol{f}_{\mathrm{v}}, \quad (23)$$

where $\boldsymbol{f}_{\mathrm{nlfk,dy}}$, $\boldsymbol{f}_{\mathrm{nlfk,st}}$ and $\boldsymbol{f}_{\mathrm{v}}$ represent the dynamic and static FK forces, and the viscous force, respectively. Note that the forces $\boldsymbol{f}_{\mathrm{d}}$, $\boldsymbol{f}_{\mathrm{r}}$, $\boldsymbol{f}_{\mathrm{g}}$ and $\boldsymbol{f}_{\mathrm{pto}}$ remain linear, as detailed in Section III.

The modelling of the non-linear FK force is well studied in [19], [33], [34] and, thus, this paper only given an overview of the methodology described in [19], [33], [34]. For heave motion, the static and dynamic non-linear FK forces can be expressed as

$$f_{\mathrm{nlfk,st},33} = -\iint_{S(t)} p_{st}\ \boldsymbol{n}\ \mathrm{d}S, \tag{24}$$

$$f_{\mathrm{nlfk,dy},33} = -\iint_{S(t)} p_{dy}\ \boldsymbol{n}\ \mathrm{d}S, \tag{25}$$

where $\boldsymbol{n}$ is the vector normal to the instantaneous wetted surface $S(t)$. The static and dynamics pressure components in the fluid are given as

$$p_{st} = -\rho g z, \tag{26}$$

$$p_{dy} = \rho g a \frac{\cosh(k(z+h))}{\cosh(kh)} \cos(\omega t - kx), \tag{27}$$

where a and k are the wave amplitude and wave number, respectively.

For the roll and pitch modes, the non-linear static and dynamic FK forces can be written as

$$f_{\mathrm{nlfk,st},ii} = -\iint_{S(t)} p_{st}\ (\boldsymbol{r} \times \boldsymbol{n})\ \mathrm{d}S, \tag{28}$$

$$f_{\mathrm{nlfk,dy},ii} = -\iint_{S(t)} p_{dy}\ (\boldsymbol{r} \times \boldsymbol{n})\ \mathrm{d}S, \tag{29}$$

where $\boldsymbol{r}$ is the position vector of the instantaneous wetted surface relative to the CoG. The symbol $\times$ represents the cross product. $ii = 44$ and $ii = 55$ represent the roll and pitch modes, respectively. Hence, the non-linear FK forces in heave, roll and pitch modes can be reformed as

$$\boldsymbol{f}_{\mathrm{nlfk,st}} = [f_{\mathrm{nlfk,st},33}, f_{\mathrm{nlfk,st},44}, f_{\mathrm{nlfk,st},55}]^{\mathrm{T}}, \tag{30}$$

$$\boldsymbol{f}_{\mathrm{nlfk,dy}} = [f_{\mathrm{nlfk,dy},33}, f_{\mathrm{nlfk,dy},44}, f_{\mathrm{nlfk,dy},55}]^{\mathrm{T}}. \tag{31}$$

In this non-linear hybrid modelling method, the concepts of 'hydrostatic restoring force' and 'excitation force' have no physical meaning. However, their counterparts, namely the 'non-linear hydrostatic restoring force' and the 'non-linear excitation force' are defined for comparison, given as

$$\boldsymbol{f}_{\mathrm{hs,nl}} = \boldsymbol{f}_{\mathrm{nlfk,st}} + \boldsymbol{f}_{\mathrm{g}}, \tag{32}$$

$$\boldsymbol{f}_{\mathrm{e,nl}} = \boldsymbol{f}_{\mathrm{nlfk,dy}} + \boldsymbol{f}_{\mathrm{d}}. \tag{33}$$

The effect of fluid viscosity on the WEC dynamics is normally represented by a quadratic drag term according to the Morrison equation [35], given as

$$f_{\mathrm{v},3} = -0.5\rho\pi R^2 C_{\mathrm{d},3}\dot{\xi}_3|\dot{\xi}_3|, \tag{34}$$

$$f_{\mathrm{v},4} = -\rho R^4 d C_{\mathrm{d},4}\dot{\xi}_4|\dot{\xi}_4|, \tag{35}$$

$$f_{\mathrm{v},5} = -\rho R^4 d C_{\mathrm{d},5}\dot{\xi}_5|\dot{\xi}_5|, \tag{36}$$

$$\boldsymbol{f}_{\mathrm{v}} = [f_{\mathrm{v},3}, f_{\mathrm{v},4}, f_{\mathrm{v},5}]^T, \tag{37}$$

where $f_{\mathrm{v},3}$, $f_{\mathrm{v},4}$ and $f_{\mathrm{v},5}$ are the viscous forces in heave, roll, pitch, with viscous coefficients $C_{\mathrm{d},3}$, $C_{\mathrm{d},4}$, and $C_{\mathrm{d},5}$, respectively.

The values of $C_{\mathrm{d},3}$, $C_{\mathrm{d},4}$ and $C_{\mathrm{d},5}$ are chosen empirically, as discussed in [36], which dependence on the Keulegan-Carpenter number, the Reynolds number and the roughness number. In practice, the viscous coefficients can be determined analytically, numerically or experimentally [25], [37], [38]. However, it is difficult to obtain consistent values if wave conditions vary significantly [39]. In this study, the values from [16] are used, with $C_{\mathrm{d},3} = 1$, $C_{\mathrm{d},4} = C_{\mathrm{d},5} = 0.7$.

To investigate the power and energy transferred from the waves to the WEC, the non-linear excitation power and energy are defined, respectively, as

$$\boldsymbol{P}_{\mathrm{e,nl}} = \boldsymbol{f}_{\mathrm{e,nl}}\dot{\boldsymbol{\xi}}, \tag{38}$$

$$\boldsymbol{E}_{\mathrm{e,nl}} = \int_0^T \boldsymbol{P}_{\mathrm{e,nl}}\ \mathrm{d}t. \tag{39}$$

V. Results and discussion

Based on the hybrid modelling method detailed in Section IV, numerical simulations are conducted to validate its capability to reveal the mutual parametric interaction between multiple DoFs. A typical monochromatic example is shown in Fig. 6, where the wave period is 6 s and the wave amplitude is 0.2 m. To focus on the mutual interaction problem, viscous and PTO forces are not considered in Fig. 6.

For the initial conditions of $\xi_3(0) = 0$ m and $\xi_4(0) = 0$ rad, parametric resonance is not triggered. In Fig. 6, the heave and roll displacements predicted by the non-linear model, considering a non-linear FK force (NLFK), and shown by the magenta curves, show no obvious differences from their linear counterparts (blue curves). However, for the initial conditions of $\xi_3(0) = 0$ m and $\xi_4(0) = 0.1$ rad, parametric resonance in roll occurs, and thus the roll angle extends to 1.2 rad, even though the wave amplitude is relatively small, at 0.2 m. In turn, this large roll motion results in a correspondingly large heave motion, with a maximum value of approx. 2.5 m. Thus, the heave and roll modes are inherently and mutually coupled, when parametric resonance occurs. Similar results are observed in [16] and thus the hybrid modelling method, with non-linear FK force representation, is capable of depicting the full extent of the parametric resonance. In addition, the onset of parametric resonance is clearly sensitive to initial condition, indicating the co-existence of multiple attractors. Such a multi-stability co-existence gives the potential for supervisory control to switch between different attractors, according to the sea state.

In Fig. 6, the heave and roll motions are unstable, with amplitude increasing as the simulation time increases. In practice, large motion in heave, roll, or/and pitch induces significant non-linear hydrodynamics, and a viscous drag term should therefore be considered. As shown in Fig. 7, parametric resonance in both roll and pitch occurs for non-linear models, as the nonlinearly modelled roll and pitch displacements are significantly larger than their linear counterparts. As the buoy heaves significantly, the metacentric height may became negative during part of a wave period, which excites the roll or/and pitch modes, causing energy transfer from heave to roll and heave to pitch.

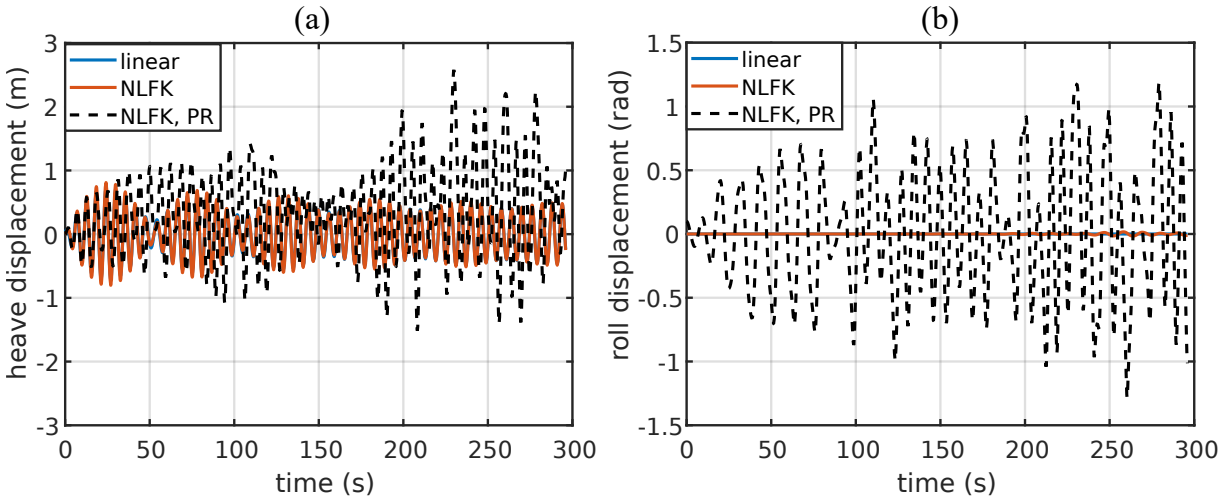

Fig. 6. The effect of initial conditions on the occurrence of parametric resonance, illustrated by the heave and roll displacements in (a) and (b), respectively. In this figure, the PTO and viscous forces are not considered.

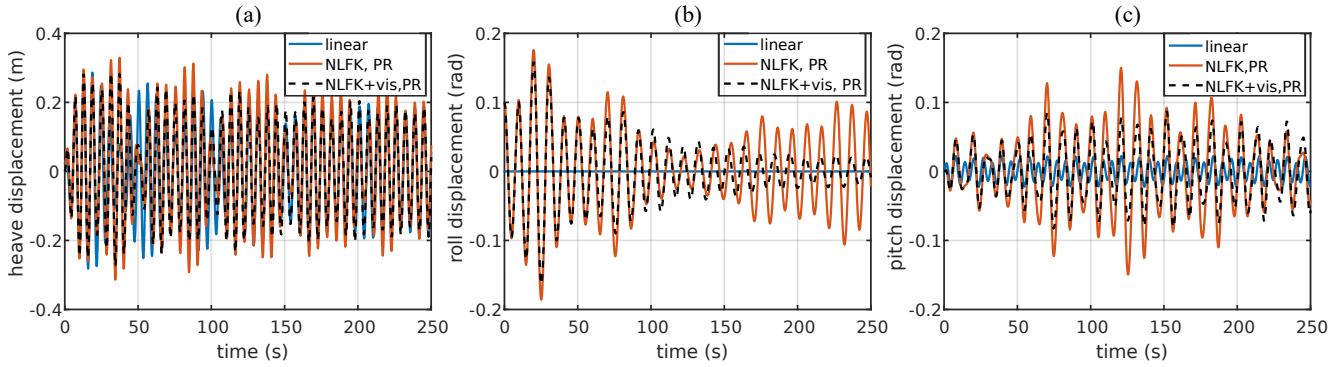

Fig. 7. Viscous effect on the parametric resonance in roll and heave, illustrated by the heave, roll and pitch displacements in (a), (b) and (c), respectively. In this figure, the PTO force is not included.

Comparing the black dashed curves with the magenta ones in Fig. 7(b), it can be concluded that the viscous force attenuates roll motion significantly, while it only slightly dampens the heave and pitch motions, as shown in Figs. 7(a) and (c), respectively. In Fig. 7, the wave period is 6.28 s, the wave amplitude is 0.1 m, and the PTO force is not included. Comparing Fig. 7 with Fig. 6 demonstrates the importance of the inclusion of viscous drag, in preventing the motion increasing to infinity.

To discus the influence of parametric resonance in WEC power/energy absorption, passive control, with a pure damping term, is implemented in the heave, roll and pitch modes, with results shown in Fig. 8. The simulation conditions correspond to a wave period of 6 s and a wave amplitude of 2 m. For the initial condition of $\xi(0) = [0, 0, 0]^T$, parametric resonance is not evident, but occurs for an initial condition of $\xi(0) = [0, 0.1, 0]^T$.

The excitation energy in heave, roll and pitch modes are shown in Figs. 8(a)-(c), respectively, with their total in Fig. 8(d). Compared to the linear model, non-linear models always show less excitation energy in heave and pitch modes. It is very interesting that the excitation energy in roll is *negative* when parametric resonance occurs, as shown in Fig. 8(c), that is, energy is dissipated. In this case, the non-linear excitation force in roll damps, rather than facilities, roll motion, causing energy loss. However, heave, pitch and total excitation energy are insensitive to the occurrence of parametric resonance.

The energy absorbed by passive PTO dampers in heave, roll and pitch modes are shown in Figs. 8(e)-(g), respectively, with their summation in Fig. 8(d). Compared to the linear model, non-linear models result in much less PTO energy absorbed from heave and pitch, with a consequently lower total PTO energy. This is expected, since viscous forces can dissipate a significant amount of energy. When parametric resonance occurs, it is possible to absorb some energy from roll, as shown in Fig. 8(f). Comparing Fig. 8(f) with Fig. 8(b), it is obvious that both the excitation energy and the PTO energy are zero when parametric resonance is not triggered. However, following the onset of parametric resonance, roll motion dissipates energy into waves, rather than harvesting energy from waves. Thus, this energy component can only come from the mutual interaction of roll with heave and pitch modes. In addition, the useful energy absorbed by the PTO damper in roll is about 2.37 kJ, to see the black dashed curve in Fig. 8(f), while the energy dissipated by the roll 'excitation force' is about 0.88 kJ. As the roll motion is small, the energy dissipated by radiation and viscous forces is relatively small. Thus, parametric resonance can transfer energy from heave

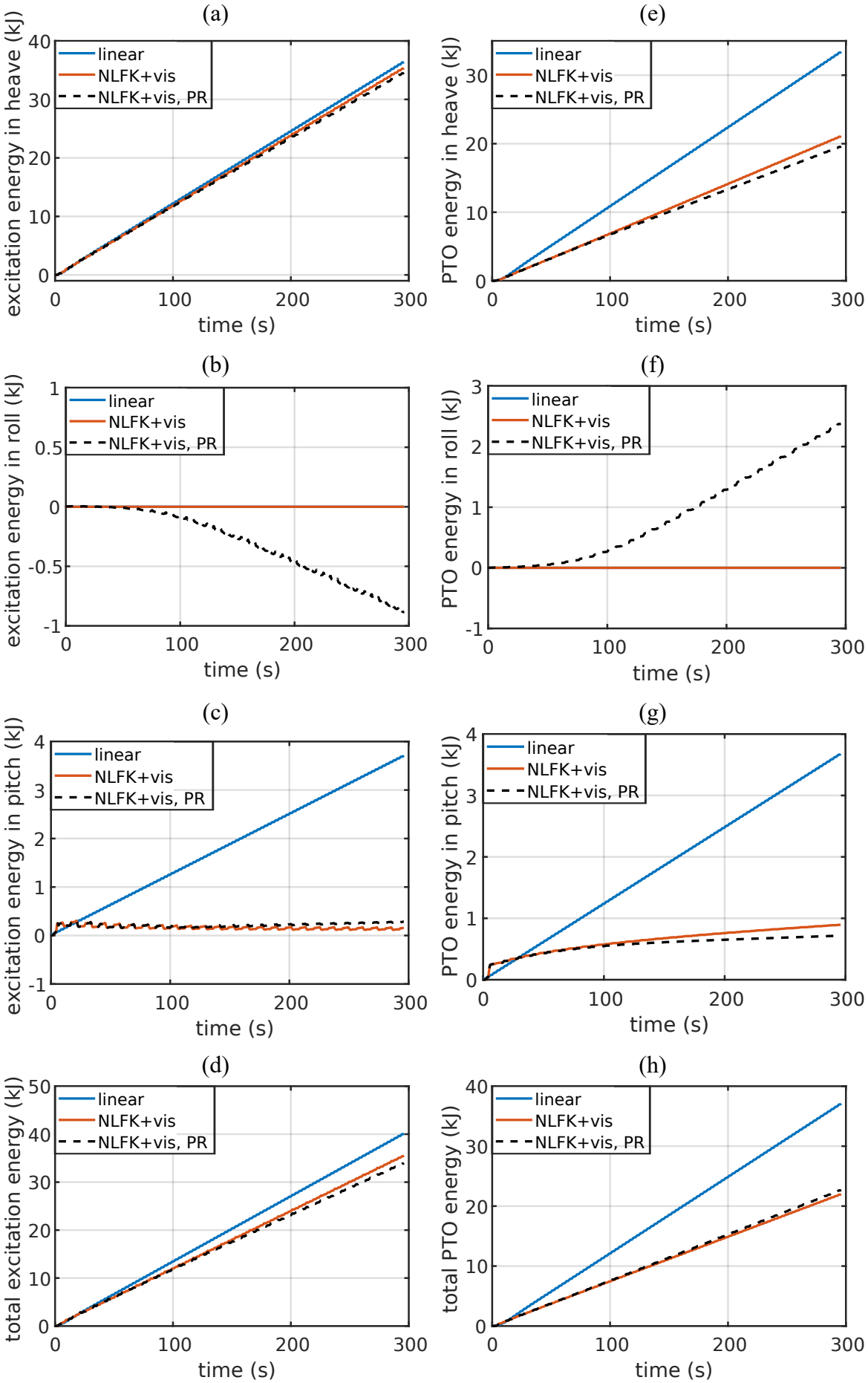

Fig. 8. Energy transfer between different DoFs illustrated by excitation energy in (a)-(d), and PTO energy in (e)-(h).

or/and pitch modes into roll mode, and then the roll PTO can absorb a large part of the transferred energy.

Although this study only reveals some preliminary insights into parametric resonance for wave energy conversion, some of findings are worth further discussion. (i) As shown in Figs. 6-8, the occurrence of parametric coupling is sensitive to initial conditions, when there coexist multiple attractors in the operational space. Further study on these basins of attraction is required to check the stability of these coexisting attractors. This may also require a high-level supervisory control system, to switch the system dynamics from one attractor to another, for triggering or suppressing parametric resonance. (ii) When parametric resonance occurs, the operation modes are mutually coupled. Overly simplistic modelling of such mutual interaction may erroneously indicate unrealistically large parametrically excited roll or pitch motion, as shown in Fig. 6, consequently resulting in overoptimistic power absorption. In such a case, accurate nonlinear hydrodynamic modelling is critical, especially when parametric resonance is triggered, as demonstrated by Figs. 6-7. (iii) For WECs which can ideally and optimally harvest energy from all DoFs, without any physical constraints, WEC power absorption approaches its theoretical limit, regardless of the occurrence of parametric resonance. However, most WEC devices are designed to harvest wave energy in one, or at most two, DoFs with stroke constraints. Pitching devices may make use of parametric resonance to absorber more power, as power in heave can be transferred to pitch, and then be absorbed by the pitch PTO system. Alternatively, it is also possible for heaving devices to spill power to roll/pitch motion via parametric resonance, especially when the heave motion exceeds the stroke constraints. However, parametric resonance is characterised by high nonlinearity, and its onset is sensitive to several factors, e.g. wave conditions, WEC hull geometry, mooring design, and the nature of the control/PTO systems, more in-depth investigation is needed.

VI. Conclusion

This study uses a simple cylindrical point absorber in heave/roll/pitch modes to investigate the energy transfer between different DoFs when parametric resonance occurs. A hybrid modelling method, considering non-linear FK and viscous forces, can effectively and efficiently model the nonlinear parametric resonance phenomenon.

Numerical simulation reveals that the heave, roll, and pitch modes are mutually coupled, when parametric resonance occurs, and overly simplistic modelling methods may lead to overoptimistic WEC motion and power absorption. Quadratic viscous terms can constrain WEC motion in some regions of the operational space, but also potentially spill a significant amount of energy, resulting in much less power abortion than indicated by linear models. When parametric resonance occurs, the roll mode cannot harvest energy from wave, but rather dissipates energy to the surrounding water, and thus this energy component is transferred from the heave or/and pitch modes, and then partly absorbed by the roll PTO system. However, the total excitation energy and PTO energy are insensitive to the onset of parametric resonance.

Ongoing work focuses on more accurately quantifying the energy transfer from one DoF to another via parametric resonance, with a view to identifying the virtue of exploiting parametric resonance in real WECs which have physical displacement limits. The study of appropriate supervisory control, used to position the device operation within desirable regions of the operational space, also deserves further study.

Acknowledgement

This project has received funding from the European Union's Horizon 2020 research and innovation programme under the Marie Skłodowska-Curie grant agreement No. 841388 and Science Foundation Ireland under Grant No. 12/RC/2302_P2 for the Marine and Renewable Energy Ireland (MaREI) centre.

References

[1] M. Sharma, E. H. Sarraf, R. Baskaran, and E. Cretu, "Parametric resonance: Amplification and damping in mems gyroscopes," *Sensors and Actuators A: Physical*, vol. 177, pp. 79–86, 2012.

[2] T. Yildirim, M. H. Ghayesh, W. Li, and G. Alici, "Design and development of a parametrically excited nonlinear energy harvester," *Energy Conversion and Management*, vol. 126, pp. 247–255, 2016.

[3] T. Fossen and H. Nijmeijer, *Parametric resonance in dynamical systems*. Springer Science & Business Media, 2011.

[4] A. Olvera, E. Prado, and S. Czitrom, "Parametric resonance in an oscillating water column," *Journal of Engineering Mathematics*, vol. 57, no. 1, pp. 1–21, 2007.

[5] R. Gomes, J. Ferreira, S. R. de Silva, J. Henriques, and L. Gato, "An experimental study on the reduction of the dynamic instability in the oscillating water column spar buoy," in *Proceedings of the 12th European Wave and Tidal Energy Conference, Cork, Ireland*, vol. 27, 2017.

[6] G. Giorgi and J. V. Ringwood, "Articulating parametric resonance for an owc spar buoy in regular and irregular waves," *Journal of Ocean Engineering and Marine Energy*, vol. 4, no. 4, pp. 311–322, 2018.

[7] G. Giorgi, R. P. Gomes, J. C. Henriques, L. M. Gato, G. Bracco, and G. Mattiazzo, "Detecting parametric resonance in a floating oscillating water column device for wave energy conversion: Numerical simulations and validation with physical model tests," *Applied Energy*, vol. 276, p. 115421, 2020.

[8] K. R. Tarrant, "Numerical modelling of parametric resonance of a heaving point absorber wave energy converter," Ph.D. dissertation, Trinity College Dublin, 2015.

[9] S. Zou, O. Abdelkhalik, R. Robinett, U. Korde, G. Bacelli, D. Wilson, and R. Coe, "Model predictive control of parametric excited pitch-surge modes in wave energy converters," *International journal of marine energy*, vol. 19, pp. 32–46, 2017.

[10] I. Kovacic, R. Rand, and S. Mohamed Sah, "Mathieu's equation and its generalizations: overview of stability charts and their features," *Applied Mechanics Reviews*, vol. 70, no. 2, 2018.

[11] T. Iseki and P. Xu, "Experimental study on coupled motions of a spar-buoy under mathieu instability," in *International Conference on Offshore Mechanics and Arctic Engineering*, vol. 58899. American Society of Mechanical Engineers, 2019, p. V010T09A027.

[12] G. Giorgi, R. P. Gomes, G. Bracco, and G. Mattiazzo, "Numerical investigation of parametric resonance due to hydrodynamic coupling in a realistic wave energy converter," *Nonlinear Dynamics*, vol. 101, no. 1, pp. 153–170, 2020.

[13] ——, "The effect of mooring line parameters in inducing parametric resonance on the spar-buoy oscillating water column wave energy converter," *Journal of Marine Science and Engineering*, vol. 8, no. 1, p. 29, 2020.

[14] H. Yang and P. Xu, "Effect of hull geometry on parametric resonances of spar in irregular waves," *Ocean engineering*, vol. 99, pp. 14–22, 2015.

[15] J. Palm, C. Eskilsson, and L. Bergdahl, *Parametric excitation of moored wave energy converters using viscous and non-viscous CFD simulations*. Taylor & Francis Group: Abingdon, UK, 2018.
[16] H. Haslum, "Simplified methods applied to nonlinear motion of spar platforms [phd dissertation]," Ph.D. dissertation, 2000.
[17] K. Tarrant and C. Meskell, "Investigation on parametrically excited motions of point absorbers in regular waves," *Ocean Engineering*, vol. 111, pp. 67–81, 2016.
[18] J. Davidson and T. Kalmár-Nagy, "A real-time detection system for the onset of parametric resonance in wave energy converters," *Journal of Marine Science and Engineering*, vol. 8, no. 10, p. 819, 2020.
[19] G. Giorgi and J. V. Ringwood, "Analytical representation of nonlinear Froude-Krylov forces for 3-DoF point absorbing wave energy devices," *Ocean Eng.*, vol. 164, pp. 749–759, 2018.
[20] J. Davidson, R. P. Gomes, R. Galeazzi, and J. C. Henriques, "Blowing the top on parametric resonance: Relief valve control for the stabilisation of an owc spar buoy," in *ASME 2020 39th International Conference on Ocean, Offshore and Arctic Engineering*. American Society of Mechanical Engineers Digital Collection, 2020.
[21] L. D. Zavodney, A. Nayfeh, and N. Sanchez, "The response of a single-degree-of-freedom system with quadratic and cubic nonlinearities to a principal parametric resonance," *Journal of Sound and Vibration*, vol. 129, no. 3, pp. 417–442, 1989.
[22] C. A. Rodríguez and M. A. Neves, "Nonlinear instabilities of spar platforms in waves," in *International Conference on Offshore Mechanics and Arctic Engineering*, vol. 44915. American Society of Mechanical Engineers, 2012, pp. 605–614.
[23] J. Falnes, *Ocean Waves and Oscillating Systems: Linear Interactions Including Wave-Energy Extraction*. Cambridge University Press, 2002.
[24] T. Pérez and T. Fossen, "Time-vs. frequency-domain identification of parametric radiation force models for marine structures at zero speed," *Modeling, Identification and Control*, vol. 29, no. 1, pp. 1–19, 2008.
[25] B. Guo, R. Patton, S. Jin, J. Gilbert, and D. Parsons, "Nonlinear modeling and verification of a heaving point absorber for wave energy conversion," *IEEE Trans. Sustain. Energy*, vol. 9, no. 1, pp. 453–461, 2017.
[26] T. Perez and T. Fossen, "A Matlab toolbox for parametric identification of radiation-force models of ships and offshore structures," *Modeling, Identification and Control*, vol. 30, no. 1, pp. 1–15, 2009.
[27] N. Faedo, Y. Peña-Sanchez, and J. V. Ringwood, "Finite-order hydrodynamic model determination for wave energy applications using moment-matching," *Ocean Eng.*, vol. 163, pp. 251–263, 2018.
[28] Y. Pena-Sanchez, N. Faedo, M. Penalba, G. Giorgi, A. Mérigaud, C. Windt, D. G. Violini, L. Wang, and J. V. Ringwood, "Finite-order hydrodynamic approximation by moment-matching (foamm) toolbox for wave energy applications," in *Proc. European Wave and Tidal Energy Conferebce*, Naples, Italy, 2019, pp. 1–9.
[29] Z. Yu and J. Falnes, "State-space modelling of a vertical cylinder in heave," *Appl. Ocean Res.*, vol. 17, no. 5, pp. 265–275, 1995.
[30] B. Guo, R. Patton, and S. Jin, "Identification and validation of excitation force for a heaving point absorber wave energy convertor," in *Proc. European Wave and Tidal Energy Conferebce*, Cork, Ireland, 2017, pp. 1–9.
[31] B. Guo, R. J. Patton, S. Jin, and J. Lan, "Numerical and experimental studies of excitation force approximation for wave energy conversion," *Renew. Energy*, vol. 125, pp. 877–889, 2018.
[32] Y. Peña-Sanchez, C. Windt, J. Davidson, and J. V. Ringwood, "A critical comparison of excitation force estimators for wave-energy devices," *IEEE Trans. Control Syst. Technol.*, pp. 2263–2275, 2019.
[33] M. Penalba Retes, A. Mérigaud, J.-C. Gilloteaux, and J. Ringwood, "Nonlinear Froude-Krylov force modelling for two heaving wave energy point absorbers," in *Proc. European Wave and Tidal Energy Conference*, Nantes, France, 2015, pp. 1–10.
[34] G. Giorgi and J. V. Ringwood, "Computationally efficient nonlinear Froude–Krylov force calculations for heaving axisymmetric wave energy point absorbers," *J. Ocean Eng. Mar. Energy*, vol. 3, no. 1, pp. 21–33, 2017.
[35] J. R. Morison, J. W. Johnson, and S. A. Schaaf, "The force exerted by surface waves on piles," *Journal of Petroleum Technology*, vol. 2, no. 05, pp. 149–154, 1950.
[36] O. T. Gudmestad and G. Moe, "Hydrodynamic coefficients for calculation of hydrodynamic loads on offshore truss structures," *Marine Structures*, vol. 9, no. 8, pp. 745–758, 1996.
[37] S. Jin, R. J. Patton, and B. Guo, "Viscosity effect on a point absorber wave energy converter hydrodynamics validated by simulation and experiment," *Renew. energy*, vol. 129, pp. 500–512, 2018.
[38] ——, "Enhancement of wave energy absorption efficiency via geometry and power take-off damping tuning," *Energy*, vol. 169, pp. 819–832, 2019.
[39] G. Giorgi and J. Ringwood, "Consistency of viscous drag identification tests for wave energy applications," in *Proc. European Wave and Tidal Energy Conference*, Cork, Ireland, 2017, pp. 1–8.